




ENSO/SAM interactions during the middle and late Holocene

The Holocene
22(1) 23–30
© The Author(s) 2011
Reprints and permission:
sagepub.co.uk/journalsPermissions.nav
DOI: 10.1177/0959683611405241
hol.sagepub.com


**Basil Gomez,¹ Lionel Carter,² Alan R. Orpin,³
Kim M. Cobb,⁴ Michael J. Page,⁵ Noel A. Trustrum⁵
and Alan S. Palmer⁶**

Abstract

A new chronology of large magnitude rainfall events derived from the continuous high-resolution Lake Tutira storm sediment record covers the last 6800 years and provides the first insight into changes in El Niño-Southern Oscillation (ENSO) teleconnections to the higher southern latitudes to be obtained from New Zealand. Synthesis with independent paleoclimate records from the tropical Pacific and Antarctica also reveals a millennial-scale waxing and waning of the teleconnections that were not visible in the narrow historical window previously used to view interactions between ENSO and the Southern Annular Mode (SAM). Consistent with modern ENSO behaviour, we find teleconnections to the Southwest Pacific throughout the middle and late Holocene, depending on the strength and phase of ENSO and the phase of the SAM. We suggest that precession-driven changes in the seasonal cycle of solar radiation exert a first-order control on the interaction between the two climate modes. Consequently, their present status may neither be indicative of conditions that prevailed earlier in the Holocene, nor of those that might be associated with future climate changes in the Southern Hemisphere extratropics.

Keywords

climate modes, El Niño-Southern Oscillation (ENSO), New Zealand, South Pacific, Southern Annular Mode (SAM), teleconnections

Introduction

A coherent picture of El Niño-Southern Oscillation (ENSO) variability in the tropical Pacific is emerging (Cane, 2005), but comparatively little is known about the impact ENSO has on the mid-latitudes of the South Pacific, where the Southern Annular Mode (SAM) also exerts an important influence on climate (Fogt and Bromwich, 2006; Kidston et al., 2009). The SAM is a product of internal atmospheric variability that reflects changes in the meridional pressure gradient between the southern mid and high latitudes, and the position and strength of the mid-latitude westerly winds. In its positive (negative) phase the SAM is associated with positive (negative) mid-latitude and negative (positive) high-latitude pressure anomalies and a stronger (weaker) westerly circumpolar flow. Since the middle of the twentieth century the positive phase of the SAM has become increasingly dominant in the austral summer (Marshall, 2003), but proxy records of the SAM's variability are limited to centennial timescales and the forcing mechanisms that give rise to observed trends are not fully understood (Fogt et al., 2009; Goodwin et al., 2004). ENSO atmospheric teleconnections to the mid- and high-latitude South Pacific are thought to be dependent upon the strength of coupling that exists between the low- and high-latitude climate modes, as well as the strength of ENSO variability (Fogt and Bromwich, 2006; Lachlan-Cope and Connolley, 2006; L'Heureux and Thompson, 2006). The coupling between ENSO and the SAM appears to have strengthened in recent decades, but current knowledge of these interactions is limited to observational and isotope records spanning the last few centuries (Fogt and Bromwich, 2006; Gregory and Noone, 2008), and longer-term

interactions between the two climate modes have yet to be resolved. Determining the manner in which these interactions evolve is key to constraining the response that southern mid- and high-latitude climate had to past ENSO variability and to making future climate projections (Watterson, 2009).

Its remote position in the middle latitudes of the South Pacific Ocean, athwart the westerly zonal circulation and peripheral to the easterly Trade Winds, makes New Zealand (NZ) an ideal location from which to examine the influence that ENSO and the SAM exert on mid-latitude climate. Observations and reanalysis data (which simulate multiple climate variables) show that variations in the southern Pacific atmospheric circulation associated with both ENSO and the SAM have a profound effect on NZ rainfall (Ummerhofer and England, 2007; Ummerhofer et al., 2009). Proxy records also suggest that ENSO likely had a strong influence on NZ climate during the late Holocene (Shulmeister et al.,

¹University of Hawai'i at Mānoa, USA

²Victoria University of Wellington, New Zealand

³National Institute of Water and Atmospheric Research, New Zealand

⁴Georgia Institute of Technology, USA

⁵GNS Science, New Zealand

⁶Massey University, New Zealand

Received 27 October 2010; revised manuscript accepted 15 February 2011

Corresponding author:

Basil Gomez, Department of Geography, University of Hawai'i at Mānoa, Honolulu HI 96822, USA.
Email: basilg@hawaii.edu

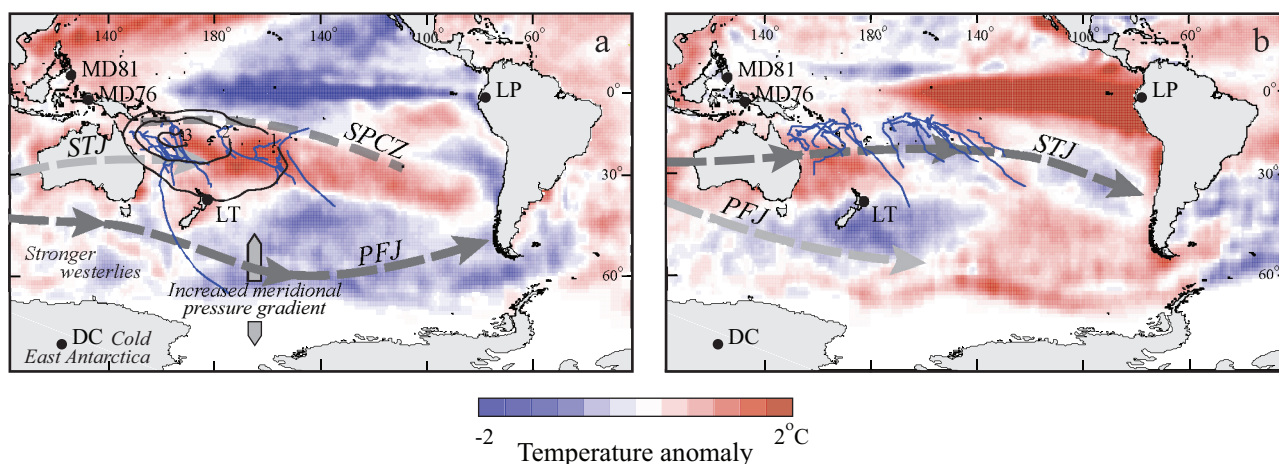


Figure 1. Location of the paleoclimate records used in this study and atmospheric influences on the South Pacific region. MD98-2181 and MD98-2176 are core sites in the Western Pacific Warm Pool (Stott et al., 2004); LP, Laguna Pallcacocha, Ecuador (Moy et al., 2002); LT, Lake Tutira, New Zealand; and DC, EPICA Dome C, Antarctica (Masson-Delmotte et al., 2004). Sea-surface temperature (SST) anomalies ($\pm^{\circ}\text{C}$ on scale bar) for December 1998 and 1997 characterize (a) La Niña and (b) El Niño conditions, respectively. The anomalies were computed with reference to the 1982 to 1998 December average derived from Reynolds' reconstructed SST data (http://ferret.pmel.noaa.gov/thredds/dodsC/NVODS/reynolds_sst_wk/data_ferret.pmel.noaa.gov/thredds_dodsC_data_PMEL_reynolds_sst_wk.nc.jnl.html last accessed 23 May 2011). Dashed lines denote the schematic locations of the subtropical (STJ) and polar front (PFJ) jets (Yuan, 2004), and the average position (1958–1998) position of the South Pacific Convergence Zone (SPCZ) during the austral summer (Folland et al., 2002). The tracks of (extra) tropical cyclones that formed in the southwest Pacific in the 1998–1999 and 1997–1998 seasons are also shown (<http://australiasevereweather.com/cyclones/> last accessed 23 May 2011). In (a), contours denote the average (1970–1997) number of cyclones passing within 555 km of each point every year (Sinclair, 2002), and annotations refer to conditions experienced during the Southern Annular Mode's positive phase

2006), and provide evidence that Antarctic influences transmitted by the westerly winds had an effect on New Zealand's paleoclimate (Williams et al., 2010). In this paper we use the high resolution sediment record from Lake Tutira, New Zealand, in conjunction with other published paleoclimate records resolved from lake, marine and ice cores, which span the South Pacific from the equator to pole (Figure 1), to investigate Southern Hemisphere climate behaviour. Synthesis of these records shows how ENSO and the SAM may have interacted to influence the frequency of large rainfall events that impacted the Eastern North Island (ENI) of NZ during the middle and late Holocene.

The Lake Tutira sediment record

Lake Tutira (39.223°S, 176.890°E) was formed by a coseismic landslide at ~ 7200 cal. yr BP (Orpin et al., 2010), and podocarp-broadleaved forest originally covered the 32 km² catchment surrounding the lake (McGlone, 2002). Humans used fire to destroy the native forests from ~ 500 cal. yr BP, and the conversion of fern and scrub to pasture commenced after European settlers arrived in AD 1873. Major rainstorms periodically inject large amounts of sediment into the lake, most of which is generated by shallow landslides (Page et al., 1994). Sediment cores have yielded a complete stratigraphy for the period of European settlement and two long (~ 2250 and ~ 7000 yr), high resolution records of storm activity (Eden and Page, 1998; Page et al., 1994, 2010). The amount of sediment generated by individual storms increased after both anthropogenic perturbations to the vegetation cover (Page et al., 1994). However, the rainfall patterns which drive sediment fluxes are determined by the atmospheric circulation and, like the rest of the ENI (Kidson and Renwick, 2002; Ummenhofer and England, 2007), rainfall events at Lake Tutira are influenced by moisture-bearing easterly to northeasterly airflows and circulation changes associated with ENSO and the SAM.

Climate modes and rainfall

El Niño (La Niña) is characterized by warm (cold) sea-surface temperature (SST) anomalies in the central and eastern equatorial Pacific, and weaker SST anomalies of opposite sign in the western equatorial Pacific (Figure 1). The different phases of ENSO influence precipitation patterns in NZ by altering the position and strength of the polar and subtropical jet streams and the path of mid-latitude storm tracks (Folland et al., 2002; Yuan, 2004). La Niña generally brings more frequent easterly to northeasterly winds and wetter than normal conditions to the ENI, whereas El Niño is typically associated with an enhanced westerly airflow and cooler, drier conditions (Kidson and Renwick, 2002; Ummenhofer and England, 2007). ENSO also affects the genesis, trajectory and frequency of tropical cyclones in the Southwest Pacific (Sinclair, 2002). Most tropical cyclones form in the austral summer when the South Pacific Convergence Zone (SPCZ) is strongest. The SPCZ is linked to the Inter-Tropical Convergence Zone (ITCZ) over the Western Pacific Warm Pool (WPWP) (Folland et al., 2002). During La Niña, when the SPCZ is displaced southwest of its average position, more tropical cyclones tend to form and transition west of longitude 180° and are able to retain their intensity over the mid-latitude Pacific Ocean and Tasman Sea (Figure 1a), where their impact on the ENI may be enhanced by NZ's orography (Sinclair, 2002). Records indicate that during the latter half of the twentieth century ENSO teleconnections to the South Pacific were amplified when La Niña (El Niño) conditions coincided with a positive (negative) SAM during the austral spring and summer, and became weaker during La Niña when ENSO was out of phase with the SAM (Fogt and Bromwich, 2006).

The SAM exerts a powerful influence on Antarctic climate (Marshall, 2007). Changes in the SAM can explain as much as 50% of the total temperature variability across Antarctica, and it has been shown that natural variability in the atmospheric circulation over the Southern Ocean is imprinted on the SAM-temperature

relation for East Antarctica (Marshall et al., 2009; Schneider et al., 2006). During the SAM's positive phase East Antarctica cools, the westerly winds over the Southern Ocean strengthen and storm tracks shift poleward (Figure 1a). A positive SAM also enhances the easterly to northeasterly airflow pattern across NZ and brings generally wetter conditions to the ENI (Gallego et al., 2005; Gillet et al., 2006; Kidston et al., 2009; Ummenhofer and England, 2007).

Core LT24

Piston core LT24 contains >1400 clay layers and sand-silt-clay graded beds ≥ 0.5 mm thick that provide an uninterrupted ~ 7000 yr long record of storm-driven erosional activity on hillslopes in the Lake Tutira catchment (Orpin et al., 2010; Page et al., 2010). LT24 was obtained ≤ 10 m from the location of core LT15, which has been the focus of efforts to evaluate paleostorm magnitude (Eden and Page, 1998; Page et al., 1994). Core chronologies rely on linear interpolation between well-established tephra dates supplemented by radiocarbon ages with uncertainties of ± 100 yr (Eden and Page, 1998; Orpin et al., 2010). The event stratigraphy in the historic period is contingent on observed rainfall. Sediment layer thickness is influenced by the sediment-delivery ratio, rate of soil recovery and land use, and varies with total rainfall over time because the dispersal system is sensitive to changes in vegetation cover (Page et al., 1994). Storm magnitude also helps determine whether shallow landsliding or sheet erosion dominates, as well as the depth of eroded regolith (Orpin et al., 2010; Page et al., 2010). Graded beds represent large magnitude rainstorms, clay layers smaller storms, and sediment layer thickness correlates well with storm magnitude (Eden and Page, 1998; Page et al., 1994). Total storm rainfall ≥ 300 mm enhances connectivity between pastoral hillslopes and stream channels and mobilizes enough sediment to produce a significant depositional response throughout the 1.8 km² lake (Page et al., 1994), and the equivalent layer thickness is 11 mm (Figure 2). Prior to European arrival it is estimated that the same rainfall total would only have generated a 3 mm thick deposit (Eden and Page, 1998).

Observations of rainfall at Tutira began in November 1894, and 10 of the 13 storms with total rainfall >300 mm that occurred between AD 1895 and 1950 can be correlated with sediment layers in LT24. (Although candidate layers exist, we could not unequivocally identify the signature of the three remaining long duration, low intensity rainstorms in the sediment record.) In the remainder of the core, which postdates the 6835 cal. yr BP *Unit G* (*Motutere*) tephra (Lowe et al., 2008), there are 233 clay layers and 154 graded beds ≥ 3 mm thick. We interpret this coherent assemblage of 397 terrigenous sediment layers to be the product of the largest rainfall events that occurred over the past 6800 yr. Except for the last ~ 500 yr of human occupation, this is a record of natural environmental variability.

Historical reconstructions of ENSO and SAM variability provide a means of contextualizing the Lake Tutira record beyond the period covered by the currently used indices. Comparison with Gergis and Fowler's (2005) and Fogt's (2007) reconstructions for the instrumental period suggests that between 1890 and 1990: (1) most (78%) of the largest sediment-producing rainstorms (>300 mm total storm rainfall) to affect the catchment between 1890 and 1990 either occurred during La Niña, when local average annual rainfall was 10% above normal, and/or at times when the SAM was in its positive phase; and (2) the majority (80%) of the most intense storms (>400 mm of rain in 72 h) occurred when La Niña conditions coincided with a positive SAM (Figure 3).

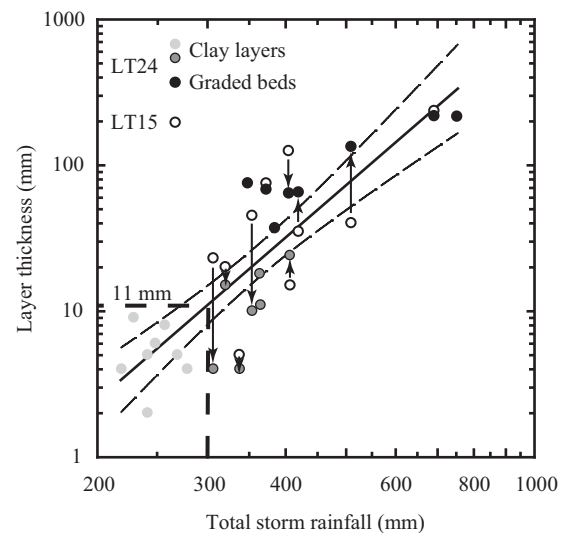


Figure 2. Relationship between sediment layer thickness and measured total storm rainfall at Lake Tutira. $R^2 = 0.7$ and dashed lines show 95% confidence intervals. Cores LT15 and LT24 were obtained from sites <10 m apart (Eden and Page, 1998; Page et al., 2010). Data points without a border denote storms recorded in LT24 that are below the present-day 300 mm (of total storm) rainfall threshold required to produce a significant depositional response throughout Lake Tutira (Page et al., 1994). Large magnitude storms that can be correlated between the two cores are represented by overlapping data points and data points linked by arrows

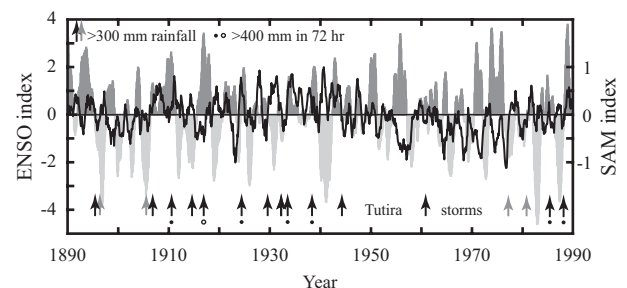


Figure 3. Comparison between reconstructions of ENSO and SAM conditions in the instrumental period and the occurrence of large magnitude storms at Lake Tutira (indicated by arrows and circles). ENSO index (gray shading, after Gergis and Fowler (2005)) and SAM index (solid black line, after Fogt (2007)). Gray arrows call attention to large magnitude storms that occurred during El Niño and/or when the SAM was positive and the open circle an intense storm that occurred when ENSO and the SAM were out of phase (see text for discussion)

To assess the extent to which large magnitude storms in the pre-observational period were coeval with La Niña we compared the centennial trend in the number of events recorded in Lake Tutira to the number of strong, very strong and extreme La Niña years documented in Gergis and Fowler's (2009) ~ 500 yr long multiproxy reconstruction of ENSO events. Other components of the atmospheric circulation influence ENI rainfall (Ummenhofer and England, 2007; Ummenhofer et al., 2009), and there is a lower level of event capture in Lake Tutira because a rainfall threshold must be crossed before landsliding engenders a significant depositional response (Page et al., 1994). However, the trend in the La Niña reconstruction is preserved (Figure 4). Thus, although the influence of a range of climate drivers is seen in the

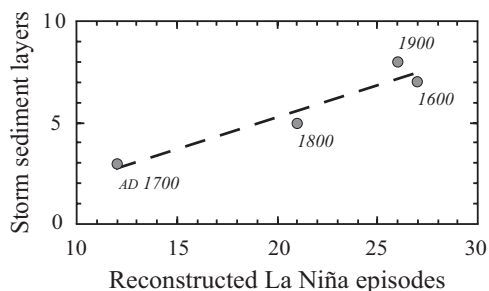


Figure 4. Relationship between the number of strong, very strong and extreme La Niña episodes in an annually resolved, multiproxy reconstruction for the pre-observational period (Gergis and Fowler, 2009) and the number of sediment layers in Lake Tutira created by large magnitude storms ($R^2 = 0.91$). The data points represent the number of La Niña episodes and storm sediment layers in 100 yr bins from AD 1550 to 1950 and figures in italics denote the bin-midpoints

Lake Tutira storm sediment record as a whole (Eden and Page, 1998; Page et al., 2010), we suggest that the assemblage of 397 sediment layers created by large magnitude storms can best be understood as a local manifestation of the large-scale climate variability associated with La Niña events and their relation with the SAM. We created an event histogram for these large magnitude storms using a bin width of 100 yr (Figure 5a).

ENSO teleconnections to the Southwest Pacific

Lake Tutira records prominent fluctuations in the frequency of large sediment-producing storms from the mid to late Holocene (from ≤ 4 to ≥ 16 events per 100 yr between ~ 5000 and ~ 2000 cal. yr BP), which are broadly similar to the trends documented by debris flow deposits in Laguna Pallcacocha, Ecuador (Moy et al., 2002) (Figure 5a, b). The trend towards higher event frequency in both lake sediment records is broadly consistent with the progressive mid- to late-Holocene intensification of ENSO as simulated by the Zebiak-Cane model (Figure 5c). Reconstructions of ENSO characteristics from tropical fossil coral sequences suggest ENSO had a lower variance at ~ 6000 cal. yr BP (Figure 5c), when precession altered the amplitude of the seasonal cycle (Clement et al., 2000), and abundant proxy evidence that indicates El Niño and La Niña activity increased after ~ 5000 cal. yr BP (Donders et al., 2008). To ascertain when statistically significant transitions occurred in the normalized time-ordered proxy records from lakes Tutira and Pallcacocha we used cumulative sum change-point analysis (Taylor, 2000). The confidence level and the importance of each change detected are given in Table 1. The critical value for a one-tailed test was used to gauge the significance level (α) of Spearman's rank order correlation coefficient and quantify the associations between different records over discrete time periods.

A level 1 change (the first change detected) in the Lake Tutira record occurs at 4900 cal. yr BP (Table 1), and there is a significant shift in the relation between the Lake Tutira and Lake Pallcacocha records at this time. Between 4900 and 2100 cal. yr BP the Lake Tutira and Laguna Pallcacocha records are positively correlated ($\alpha = 0.01$), after 2100 cal. yr BP they are negatively correlated ($\alpha = 0.01$), and before 4900 cal. yr BP we accept the null hypothesis that there is no correlation between the two records (Figure 5a, b). We suggest that the association between

the two storm records varies over time because the Lake Tutira signal reflects the dual influence both ENSO and the SAM exert on NZ rainfall; whereas rainfall at Laguna Pallcacocha is primarily ENSO forced (Moy et al., 2002). To investigate this possibility and index the behaviour of ENSO and the SAM over the last 7000 yr we use the Mg/Ca paleothermometry for cores MD98-2181 and MD98-2176 from the WPWP (Stott et al., 2004), and the stable isotope temperature estimates for the EPICA Dome C ice core (Masson-Delmotte et al., 2004) (Figure 1). These temperature proxies provide evidence of long-term changes in the mean state and variability of the tropical Pacific and Antarctic, respectively. Our use of the Dome C isotope data as an extended proxy for the SAM is predicated on the recent finding that the regional SAM-temperature relation for East Antarctica is closely linked to the atmospheric circulation pattern over the Southern Ocean (Marshall et al., 2009). That said, we also recognize that attempts to develop extended SAM time series from Antarctic ice core data are in their infancy and that the utility of these reconstructions is the subject of ongoing debate (Russell and McGregor, 2009).

There is a level 1 change in the Dome C record at 5900 cal. yr BP, signalling the transition to generally more stable temperatures that persist throughout the mid Holocene (Masson-Delmotte et al., 2004), and a concurrent change occurs in the Lake Tutira record at this time (Figure 5, Table 1). ENSO teleconnections to high southern latitudes depend upon the strength of the Hadley circulation and the intensity and position of convection in the tropics (Fogt and Bromwich, 2006; Yuan, 2004). But the SAM is able to exert a stronger influence on the mid-latitudes at times when ENSO is weak (Fogt and Bromwich, 2006), and a positive correlation ($\alpha = 0.1$) between the Lake Tutira and Dome C records implies that the ENI may have been more responsive to forcing from higher, rather than lower latitudes between 6800 and 4900 cal. yr BP. As the ITCZ transitioned south and attained its present position near the equator, and the ENSO cycle intensified ~ 5000 cal. yr BP (Koutavas and Lynch-Stieglitz, 2004; Moy et al., 2002), the connection between the low and high latitude climate modes strengthened. By 4900 cal. yr BP the ENI was strongly teleconnected to events in the tropical Pacific, and Lake Tutira and Laguna Pallcacocha register the same response to the level 1 change in the WPWP record that occurred at 4700 cal. yr BP (Figure 5, Table 1).

A further intensification of the ENSO cycle produced a contemporaneous change in the Lake Tutira and Laguna Pallcacocha records at 3350 ± 50 cal. yr BP (Figure 5a, b, c). The relation between the WPWP and Dome C temperature reconstructions also shifts at this time (Figure 5d, e); the two records are negatively correlated ($\alpha = 0.05$) from 4900 to 3300 cal. yr BP and positively correlated ($\alpha = 0.1$) from 3300 to 2100 cal. yr BP. However, there is no correlation between the two temperature records either prior to 4900 or after 2100 cal. yr BP. That is, the Lake Tutira and Laguna Pallcacocha storm records are in-phase at times when the principal modes of Southern Hemisphere atmospheric variability appear to work together, and a warm WPWP (La Niña) correlates with a cool Antarctic (+SAM) and cool WPWP (El Niño) correlates with a warm Antarctic (-SAM) (Figure 5). Conversely, the records are of opposite phase or uncorrelated at times when the temperature reconstructions we use to index the behaviour of ENSO and the SAM indicate that the two climate modes do not reinforce one another.

At times when the low- and high-latitude climate modes reinforce one another ENSO teleconnections to the South Pacific are amplified if La Niña conditions coincide with a positive SAM

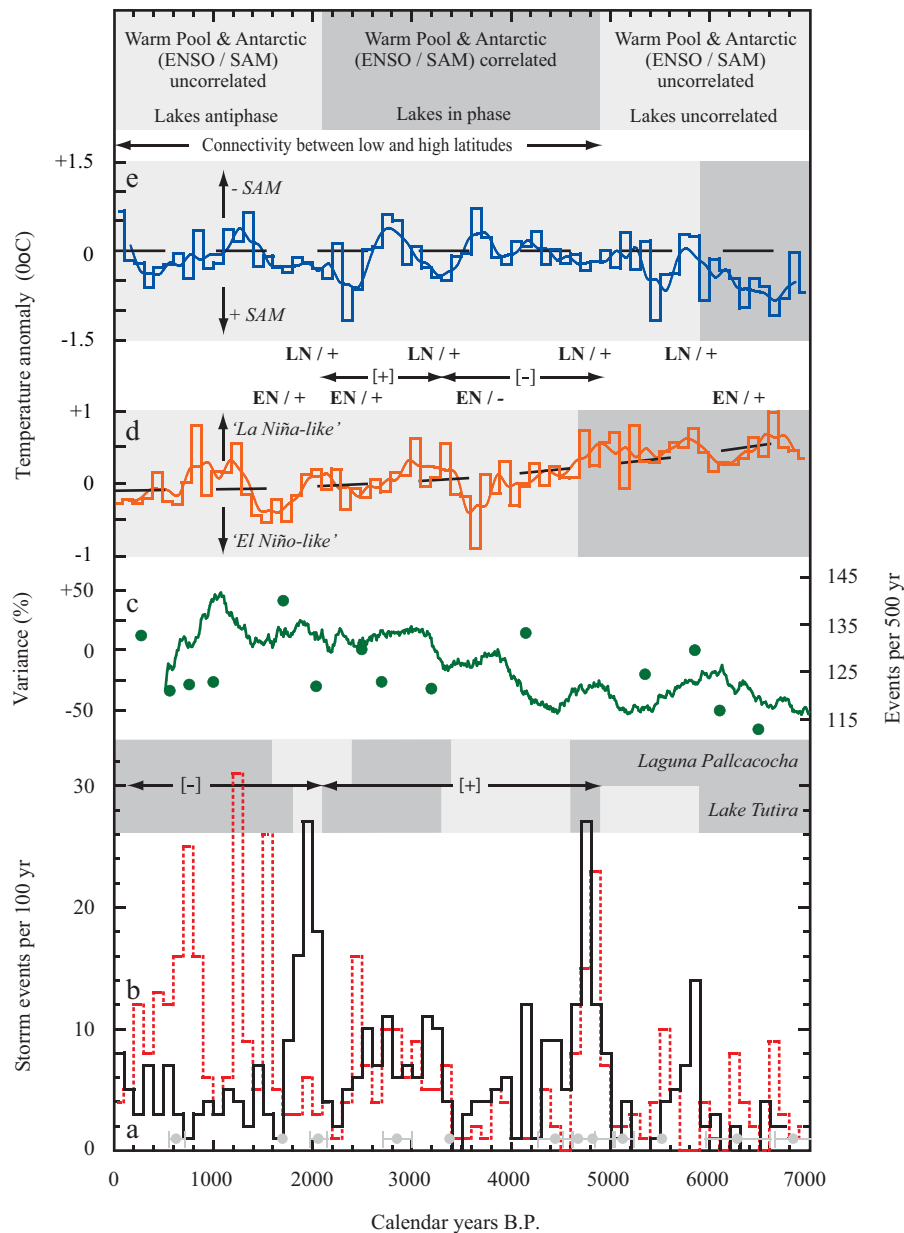


Figure 5. Comparison of the Lake Tutira core LT24 record of pale-ENSO/SAM activity with Southern Hemisphere paleoproxies (see Figure 1 for core locations) and simulated records. (a) Lake Tutira event histogram, the number of large magnitude storms in 100-yr bins, superimposed on (b), the analogous event time series for Laguna Pallcacocha, Ecuador (Moy et al., 2002). Dots with horizontal error bars indicate the locations and estimated age ranges for tephras in core LT24. (c) ENSO behaviour characterized by: an ensemble mean (solid line) of six simulations with the Zebiak-Cane model forced by orbital variations (warm events are defined as model years in which the boreal winter SST anomaly in the Niño-3 region exceeds 3°C); and the percent change (dots) in the difference between the ENSO variances of fossil and modern coral from sites on Palmyra and Christmas islands, Vanuatu and Papua New Guinea (Cobb et al., 2003; Corrège et al., 2000; McGregor and Gagan, 2003; Tudhope et al., 2001; Woodroffe et al., 2003). The fossil coral variance changes were calculated from raw data, except in the case of the statistics for corals from northern Papua New Guinea (McGregor and Gagan, 2003), which were estimated from graphs and are plotted with conservative $\pm 20\%$ error. (d) Western Pacific Warm Pool SST reconstruction derived from the Mg/Ca paleothermometry for cores MD98-2181 and MD98-2176 (Stott et al., 2004), shown as the departure of the 100-year bin average from the threshold temperature (29°C) at which strong convection is initiated over the ocean surface (the thick dashed line shows the long-term trend and the thin solid line the short-term trend as represented by a three-point moving average). (e) Central Antarctic temperature anomalies reconstructed from the stable water isotopes in the EPICA Dome C ice core (Masson-Delmotte et al., 2004) shown as a 100-yr bin average (the thin solid line shows the short-term trend as represented by a three-point moving average). Variations in grey shading denote transition points where the mean of the time-ordered data shifts (Table 1). Arrows and annotations draw attention to indicative relationships between the low and high latitude temperature records which we use to index the behaviour of ENSO and the SAM, and between the lake sediment records. Operators in square brackets indicate the sign of statistically significant relationships and bold type denotes interactions between the two climate modes that promote a strong teleconnected response in the Lake Tutira record, as discussed in the text (e.g. LN / + (EN / -) denotes La Niña (El Niño) conditions and a positive (negative) SAM)

(Fogt and Bromwich, 2006). Erosional activity at Lake Tutira invariably peaks (≥ 10 events in 100 yr) when this is the case (Figure 5a, d, e). An anomalous spike centred on 4150 cal. yr BP

may be a product of storm-generated erosion in a landscape preconditioned by a major ($M_w = 7.4$) earthquake that occurred ~ 4200 cal. yr. BP (Hayward et al., 2006). Major lulls in storm activity at

Table 1. Transition points in each specified proxy record detected by cumulative sum change-point analysis (Taylor, 2000). The confidence level is obtained by bootstrapping, and the level indicates the number of passes through the record required to detect the change (e.g. a level 1 change is the first change detected). Data binning minimizes errors in the depth–age relationships used to calibrate the proxy records, such that uncertainty in the timing of the transition points does not exceed ± 200 yr

Record	Cal. yr BP	Confidence level (%)	Level
Tutira	5900	97	3
	4900	99	1
	4600	94	8
	3300	100	5
	2100	98	6
	1800	100	4
Pallcacocha	4600	91	3
	3400	100	4
	2400	95	5
	1600	95	1
Warm Pool	4700	100	1
Dome C	5900	91	1

Lake Tutira (≤ 1 event in 100 yr) also tend to correspond with a positive SAM. However, changes in tropical Pacific SSTs influence NZ precipitation through feedbacks in the SPCZ (Carvalho et al., 2005), and there is a general coherence between anomalously cool WPWP SSTs and low storm activity (≤ 3 events in 100 yr) at Lake Tutira (Figure 5a, d). Both indices are consistent with El Niño, when cool WPWP SSTs move the centre of atmospheric convection and the zone of tropical cyclone nucleation eastward (Figure 1b), teleconnections to the South Pacific become weaker (Fogt and Bromwich, 2006), and stronger westerly airflow in the extratropics typically brings drier conditions to the ENI (Sinclair, 2002; Ummenhofer and England, 2007). Teleconnections to the South Pacific are also weaker during La Niña when ENSO is out of phase with the SAM (Fogt and Bromwich, 2006). After 2100 cal. yr BP, when this is apparently the case, fewer large magnitude storms are recorded in Lake Tutira.

Changes detected in the Lake Tutira record at 2100 and 1800 cal. yr BP bracket a cold perturbation that occurs in East Antarctic isotopic records at ~ 2000 cal. yr BP (Masson et al., 2000). The concurrent peak in storm activity (≥ 16 events per 100 yr) is consistent with the amplification of ENSO teleconnections to the South Pacific when La Niña coincides with a positive SAM (Figure 5), and a local pollen record provides independent evidence that the ENI was indeed wetter at this time (McGlone, 2002). Moreover, because ENSO and the SAM affect storms of all magnitudes, aggregate storm activity also peaks between 2100 and 1700, as well as from 3300 to 3100 and 5000 to 4600 cal. yr BP (Page et al., 2010), when the two climate modes are synchronized and the easterly and northeasterly airflows that bring moisture to the ENI dominate (Ummenhofer and England, 2007; Ummenhofer et al., 2009). Conversely, there are lacunae in aggregate storm activity, centred on 1650 and from 6500 to 6100 cal. yr BP (Page et al., 2010), when the two climate modes operate independently and El Niño coincides with a positive SAM, because convective activity in the SPCZ is reduced during the austral summer and winter storm tracks shift poleward.

Our focus is on the information contained in the Lake Tutira storm sediment record, but the change we detect in the Laguna Pallcacocha record at 2400 cal. yr. BP may be indicative of tighter coupling between the ITCZ and the Southern Oscillation in the Pacific, which is thought to have increased the variability of El Niño-related rainfall at that time (Figure 5b; Table 1) (Woodroffe

et al., 2003). The change at 1600 cal. yr BP marks the peak of ENSO activity that is a precursor to the insolation-forced decline in the frequency of moderate-to-strong El Niño events in the Laguna Pallcacocha record (Clement et al., 2000; Moy et al., 2002).

Conclusions

The presence of multiple or competing climate signals makes it difficult to extract information about the leading modes of Southern Hemisphere atmospheric variability from just a single proxy record or location. Robust comparisons are also often precluded by age model uncertainties (which, for all the records we use, do not exceed ± 200 yr). However, our synthesis of high-resolution Southern Hemisphere Holocene paleoclimate records, which span the Pacific sector of the Southern Hemisphere (Figure 1), suggests that for >6000 yr the relation between ENSO and the SAM has waxed and waned at millennial timescales (Figure 5).

ENSO history has been closely linked to precessional forcing (Cane, 2005; Clement et al., 2000), with changes in insolation seasonality apparently amplifying the ENSO cycle at ~ 5000 and ~ 2000 cal. yr BP. By altering the seasonal temperature contrast between low and high latitudes and the meridional temperature gradient, precession also exerts a first-order control on the strength and position of the southern westerly zonal circulation (Renssen et al., 2005). However, the small aggregate increases in the simulated strength of the westerly winds between 45° and 60° S that occurred after ~ 6000 and ~ 2000 cal. yr BP show a stronger dependence on the changing pattern of seasonal insolation (Renssen et al., 2005), than on the sum of annual insolation recorded by the EPICA Dome C isotopic thermometer which we use to index the SAM. We find that connectivity between low and high latitude climate increased as the ocean–atmosphere systems in the tropical Pacific and Antarctic transitioned to their present regimes in the mid Holocene. ENSO teleconnections to the extratropics appear to have been established by 4900 cal. yr BP, and to have been reconstituted at 2100 cal. yr BP (Figure 5). Consistent with observations (Fogt and Bromwich, 2006; Gregory and Noone, 2008), comparison of the ENSO-driven event chronologies from Lake Tutira and Laguna Pallcacocha shows that ENSO teleconnections to the extratropics strengthen when ENSO and the SAM are in phase (Figure 5). Thus we suggest that the relation between the two climate modes may be sensitive to precession.

The time-variations in the relation between the Lake Tutira and Laguna Pallcacocha records provide the first indication of a millennial-scale response of ENSO and SAM interactions to insolation forcing. They further suggest the recent status of the two large-scale climate modes may not be representative of conditions that prevailed at other times in the Holocene. This observation has important ramifications for unlocking the knowledge of climate variations that Antarctic paleoenvironmental records contain, because ENSO teleconnections may have forced some of the climate changes contained in these records (Das and Alley, 2008; Shevenell et al., 2011). Moreover, to understand how precipitation patterns in the middle and high southern latitudes may evolve in the future it may, for example, be necessary to account for the coupled response of ENSO and the SAM to increased levels of greenhouse gases.

Acknowledgements

This research was supported by the National Science Foundation grants SBR-907195 and BCS-0317570 to B.G., New Zealand Foundation of Science and Technology; contract C05X0701 to GNS Science; contracts C01X0203 and C01X0702 to the National Institute of Water and Atmospheric Research; and contract VICX0704 to Victoria University of Wellington. We thank Amy Clement for sharing the output of her ensemble model runs with us, and James Crampton and Euan Smith for advice on statistical analyses.

References

- Cane MA (2005) The evolution of El Niño, past and future. *Earth and Planetary Science Letters* 230: 227–240.
- Carvalho LM, Jones C and Ambrizzi T (2005) Opposite phases of the Antarctic Oscillation and relationships with intraseasonal to interannual activity in the Tropics during the austral summer. *Journal of Climate* 18: 702–718.
- Clement AC, Seager R and Cane MA (2000) Suppression of El Niño during the mid-Holocene by changes in the Earth's orbit. *Paleoceanography* 15: 731–737.
- Cobb KM, Charles CD, Edwards RL, Cheng H and Kastner M (2003) El Niño–Southern Oscillation and tropical Pacific climate during the last millennium. *Nature* 424: 271–276.
- Corrège DT, Récy J, Beck WM, Cabioch G and Le Cornec F (2000) Evidence for stronger El Niño–Southern Oscillation (ENSO) events in a mid-Holocene massive coral. *Paleoceanography* 15: 465–470.
- Das SB and Alley RB (2008) Rise in frequency of surface melting at Siple Dome through the Holocene: Evidence for increasing marine influence on the climate of West Antarctica. *Journal of Geophysical Research* 113: D02112, doi: 10.1029/2007JD008790.
- Donders T, Wagnercremer F and Visscher H (2008) Integration of proxy data and model scenarios for the mid-Holocene onset of modern ENSO variability. *Quaternary Science Reviews* 27: 571–579.
- Eden DN and Page MJ (1998) Palaeoclimatic implications of a storm erosion record from late Holocene lake sediments, North Island, New Zealand. *Palaeogeography, Palaeoclimatology, Palaeoecology* 139: 37–58.
- Fogt RL (2007) Investigation of the Southern Annular Mode and the El Niño–Southern Oscillation Interactions. Unpublished Ph.D. Dissertation, Atmospheric Sciences Program, Department of Geography, The Ohio State University, 212 pp.
- Fogt RL and Bromwich DH (2006) Decadal variability of the ENSO teleconnection to the high latitude South Pacific governed by coupling with the Southern Annular Mode. *Journal of Climatology* 19: 979–997.
- Fogt RL, Perlwitz J, Monaghan AJ, Bromwich DH, Jones JM and Marshall GJ (2009) Historical SAM variability. Part II: 20th century variability and trends from reconstructions, observations, and the IPCC AR4 Models. *Journal of Climatology* 22: 5346–5365.
- Folland CK, Renwick JA, Salinger MJ and Mullan AB (2002) Relative influences of the Interdecadal Pacific Oscillation and ENSO on the South Pacific Convergence Zone. *Geophysical Research Letters* 29: 1643 doi: 10.1029/2001GL014201.
- Gallego D, Ribera P, Garcia-Herrera R, Hernandez E and Gimeno L (2005) A new look for the Southern Hemisphere jet stream. *Climate Dynamics* 24: 607–621.
- Gergis JL and Fowler AM (2005) Classification of synchronous oceanic and atmospheric El Niño–Southern Oscillation (ENSO) events for paleoclimate reconstruction. *International Journal of Climatology* 25: 1541–1565.
- Gergis JL and Fowler AM (2009) A history of ENSO events since A.D. 1525: Implications for future climate change. *Climatic Change* 92: 343–387.
- Gillet NP, Kell TD and Jones PD (2006) Regional impacts of the Southern Annular Mode. *Geophysical Research Letters* 33: doi: 10.1029/2006GL027721.
- Goodwin ID, van Ommen TD, Curren MAJ and Mayewski PA (2004) Mid-latitude winter climate variability in the South and southwest Pacific regions since 1300 AD. *Climate Dynamics* 22: 783–794.
- Gregory S and Noone D (2008) Variability in the teleconnection between the El Niño–Southern Oscillation and West Antarctic climate deduced from West Antarctic ice core isotope records. *Journal of Geophysical Research* 113: D17110, doi: 10.1029/2007JD009107.
- Hayward BW, Grenfell HR, Sabaa AT, Carter R, Cochran U and Lipps JH et al. (2006) Micropaleontological evidence of large earthquakes in the past 7200 years in southern Hawke's Bay, New Zealand. *Quaternary Science Reviews* 25: 1186–1207.
- Kidson JW and Renwick JA (2002) Patterns of convection in the tropical Pacific and their influence on New Zealand weather. *International Journal of Climatology* 22: 151–174.
- Kidston J, Renwick JA and McGregor J (2009) Hemispheric scale seasonality of the southern annular mode and impacts on the climate of New Zealand. *Journal of Climatology* 22: 4759–4770.
- Koutavas A and Lynch-Stieglitz J (2004) Variability of the marine ITCZ over the eastern Pacific during the past 30,000 years. In: Diaz HF and Bradley RS (eds) *The Hadley Circulation: Present, Past and Future*. Dordrecht: Kluwer, 347–369.
- Lachlan-Cope T and Connolley W (2006) Teleconnections between the tropical Pacific and the Amundsen–Bellinghousens Sea: Role of the El Niño/Southern Oscillation. *Journal of Geophysical Research* 111: D23101, 10.1029/2005JD006386.
- L'Heureux ML and Thompson DWJ (2006) Observed relationships between the El-Niño/Southern Oscillation and the extratropical zonal-mean circulation. *Journal of Climatology* 19: 276–287.
- Lowe DJ, Shane PAR, Alloway BV and Newnham RM (2008) Fingerprints and age models for widespread New Zealand tephra marker beds erupted since 30,000 years ago: A framework for NZ-INTIMATE. *Quaternary Science Reviews* 27: 95–126.
- Marshall GJ (2003) Trends in the southern annular mode from observations and reanalyses. *Journal of Climatology* 16: 4134–4143.
- Marshall GJ (2007) Half-century seasonal relationships between the Southern Annular mode and Antarctic temperatures. *International Journal of Climatology* 27: 373–383.
- Marshall GJ, Di Battista S, Naik SS and Thamban M (2009) Analysis of a regional change in the sign of the SAM–temperature relationship in Antarctica. *Climate Dynamics* doi 10.1007/s00382-009-0682-9.
- Masson V, Vimeux F, Jouzel J, Morgan A, Delmotte M and Ciais P et al. (2000) Holocene climate variability in Antarctica based on 11 ice-core isotopic records. *Quaternary Research* 54: 348–358.
- Masson-Delmotte V, Stenni B and Jouzel J (2004) Common millennial-scale variability of Antarctic and Southern Ocean temperatures during the past 5000 years reconstructed from the EPICA Dome C ice core. *The Holocene* 14: 145–151.
- McGlone MS (2002) A Holocene and latest Pleistocene pollen record from Lake Poukawa, Hawke's Bay, New Zealand. *Global Planetary Change* 33: 283–299.
- McGregor HV and Gagan MK (2003) Diagenesis, geochemistry of Porites corals from Papua New Guinea: Implications for paleoclimate reconstruction. *Geochimica Cosmochimica Acta* 67: 2147–2156.
- Moy CM, Seltzer GO, Seltzer DT and Anderson DM (2002) Variability of El Niño/Southern Oscillation activity at millennial time scales during the Holocene epoch. *Nature* 420: 162–165.
- Orpin AR, Carter L, Page MJ, Cochran UA, Trustrum NA, Gomez B et al. (2010) Holocene sedimentary record from Lake Tutira: A template for upland watershed erosion proximal to the Waipaoa Sedimentary System, north-eastern New Zealand. *Marine Geology* 270: 11–29.
- Page MJ, Trustrum NA and DeRose RC (1994) A high resolution record of storm-induced erosion from lake sediments, New Zealand. *Journal of Paleolimnology* 11: 333–348.
- Page MJ, Trustrum NA, Orpin AR, Carter L, Gomez B, Cochran UA et al. (2010) Storm frequency and magnitude in response to Holocene climate variability, Lake Tutira, north-eastern New Zealand. *Marine Geology* 270: 30–44.
- Renssen H, Goosse H, Fichefet T, Masson-Delmotte V and Koç N (2005) Holocene climate evolution in the high-latitude Southern Hemisphere simulated by a coupled atmosphere–sea ice–ocean–vegetation model. *The Holocene* 15: 951–964.

- Russell A and McGregor GR (2009) Southern Hemisphere atmospheric circulation: Impacts on Antarctic climate and reconstructions from Antarctic ice core data. *Climatic Change* doi: 10.1007/s10584-009-9673-4.
- Schneider DP, Steig EJ, van Ommen TD, Dixon DA, Mayewski PA, Jones JM et al. (2006) Antarctic temperatures over the past two centuries from ice cores. *Geophysical Research Letters* 33: L16707, doi: 10.1029/2006GL027057.
- Shevenell AE, Ingalls AE, Domack EW and Kelly C (2011) Holocene Southern Ocean surface temperature variability west of the Antarctic Peninsula. *Nature* 470: 250–254.
- Shulmeister J, Rodbell DT, Gagan MK and Seltzer GO (2006) Inter-hemispheric linkages in climate change: Paleo-perspectives for future climate change. *Climates of the Past* 2: 167–185.
- Sinclair MR (2002) Extratropical transition of southwest Pacific tropical cyclones. Part I: Climatology and mean structure changes. *Monthly Weather Review* 130: 590–609.
- Stott LD, Cannariato K, Thunell R, Haug GH, Koutavas A and Lund S (2004) Decline of surface temperature and salinity in the western tropical Pacific Ocean in the Holocene epoch. *Nature* 431: 56–59.
- Taylor W (2000) Change-point analysis: A powerful new tool for detecting changes. Available at: <http://www.variation.com/cpa/tech/changepoint.html> (last accessed 23 May 2011).
- Tudhope AW, Chilcott CP, McCulloch MT, Cook E, Chappell J and Ellam RM et al. (2001) Variability in the El Niño Southern Oscillation through a glacial–interglacial cycle. *Science* 291: 1511–1517.
- Ummenhofer CC and England MH (2007) Interannual extremes in New Zealand precipitation linked to modes of Southern Hemisphere climate variability. *Journal of Climate* 20: 5418–5440.
- Ummenhofer CC, Gupta AS and England MH (2009) Causes of late twentieth-century trends in New Zealand precipitation. *Journal of Climate* 22: 3–19.
- Watterson IG (2009) Components of precipitation and temperature anomalies and change associated with modes of the Southern Hemisphere. *International Journal of Climatology* 29: 809–826.
- Williams PW, Neil HL and Zhao J-X (2010) Age frequency distribution and revised stable isotope curves for New Zealand speleothems: Palaeoclimatic implications. *International Journal of Speleology* 39: 99–112.
- Woodroffe CD, Beech M and Gagan MK (2003) Mid–late Holocene El Niño variability in the equatorial Pacific from coral microatolls. *Geophysical Research Letters* 30: 1358, doi: 10.1029/2002GL015868.
- Yuan X (2004) ENSO-related impacts on Antarctic sea ice: A synthesis of phenomenon and mechanisms. *Antarctic Science* 16: 415–424.